Structure determination of the (1×2) and (1×3) reconstructions of Pt(110) by low-energy electron diffraction

P. Fery, W. Moritz, and D. Wolf
Institut für Kristallographie und Mineralogie,
Universität München, Theresienstrasse 41, 8000 München 2, Federal Republic of Germany
(Received 8 December 1987)

The atomic geometry of the (1×2) and (1×3) structures of the Pt(100) surface has been determined from a low-energy electron-diffraction intensity analysis. Both structures are found to be of the missing-row type, consisting of (111) microfacets, and with similar relaxations in the subsurface layers. In both reconstructions the top-layer spacing is contracted by approximately 20% together with a buckling of about 0.17 Å in the third layer and a small lateral shift of about 0.04 Å in the second layer. Further relaxations down to the fourth layer were detectable. The surface relaxations correspond to a variation of interatomic distances, ranging from −7% to +4%, where in general a contraction of approximately 3% for the distances parallel to the surface occurs. The Pendry and Zanazzi-Jona R factors were used in the analysis, resulting in a minimum value of $R_P=0.36$ and $R_{ZJ}=0.26$ for 12 beams at normal incidence for the (1×2) structure, and similar agreement for 19 beams of the (1×3) structure. The (1×3) structure has been reproducibly obtained after heating the crystal in an oxygen atmosphere of 5×10^{-6} mbar at 1200 K for about 30 min and could be removed by annealing at 1800 K for 45 min after which the (1×2) structure appeared again. Both reconstructed surfaces are clean within the detection limits of the Auger spectrometer. CO adsorption lifts the reconstruction in both structures. After desorption at 500 K the initial structures appear again, indicating that at least one of the reconstructions does not represent the equilibrium structure of the clean surface and may be stabilized by impurities.

INTRODUCTION

The (1×2) reconstruction of the (110) surfaces of Pt, Ir, and Au has been studied by a number of different methods and it is well established now that these surfaces exhibit a missing-row type of reconstruction. For the Pt(110)-(1×2) surface the details of the atomic geometry have not been determined with sufficient reliability and the origin of the reconstruction is still the subject of controversial discussion at all reconstructed metal surfaces. Recent structure analyses by low-energy electron diffraction (LEED) of the Au(110)-(1×2) (Ref. 1) and Ir(110)-(1×2) (Ref. 2) surfaces have shown that the strong distortion of the surface results in relaxations of the subsurface layers. The main feature is a buckling in the third layer probably caused by a tendency to smooth the large corrugation of the surface. Similar results have been found by other techniques. Direct observation by field ion images,[3] alkali-metal-ion scattering,[4] and Rutherford backscattering (RBS)[5,6] clearly favored the missing-row reconstruction of Pt(110) and excluded other possible models. For Au(110) the reconstruction could also be directly observed with scanning-tunneling microscopy (STM) (Ref. 7) and relaxations of interatomic distances in subsurface layers were detected by medium-energy ion scattering (MEIS),[8] low-energy ion scattering (LEIS),[9,10] and glancing-incidence x-ray diffraction.[11] In the first LEED analysis of the Pt(110)-(1×2) reconstruction[12] also a preference for the missing-row model has been found, though only poor agreement has been reached between experimental and theoretical I-V curves. In contrast to the surface of Ir and Au an expansion of the first interlayer spacing has been found. Therefore we have performed a new LEED analysis of the Pt(110)-(1×2) reconstruction, using a new experimental data set consisting of twelve I-V curves at normal incidence. In addition to earlier studies[1,2,12] atomic displacements in the first five layers of the surface have been included.

As the second point in this paper we present a LEED structure analysis of the (1×3) superstructure, which could be prepared reproducibly. In previous experimental studies the existence of a (1×3) superstructure had been reported for Au(110),[13] Ir(110) (Ref. 14), and Pt(110).[15] The conditions at which the (1×3) superstructure appears and whether it is a stable surface configuration have not become quite clear until now. Also, the cleanliness of the reconstructed surfaces has been questioned recently and either a stabilization by impurities or even a superstructure formed by adsorbed or segregated impurities has been proposed.[16] From the various results and from the LEED structure analysis a superstructure formed by adsorbates can be definitely excluded. The interpretation of the missing-row structure as the beginning of a faceting of the surface has led to the question why the Au(110), Ir(110), and Pt(110) shows usually a (1×2) reconstruction as the stable surface and not reconstructions with larger periodicities. Theoretical calculations using the effective medium theory have shown that in cases where the (1×2) reconstruction is stable the (1×3) structure is even more stable and the

(1×4) structure even more so,[17] other calculations favored the (1×2) structure.[18] The question as to which of the two reconstructions represents the stable atomic configuration in the surface and which impurities could induce the (1×2) or (1×3) reconstruction is still open, though the fact that the (1×2) structure has been reproduced under various conditions in a number of laboratories is indicative of the stability of the (1×2) structure.

EXPERIMENTAL PROCEDURES

The experiments were carried out in an ultrahigh-vacuum system with a base pressure of 5×10^{-11} mbar equipped with a four-grid LEED system and Auger-electron spectroscopy (AES). The LEED intensity spectra were measured with a computer-controlled Faraday cup. The platinum crystal of 99.999% purity has been oriented to within of 0.05° of the [1$\bar{1}$0] direction by x-ray diffraction and has been polished mechanically with 0.7-μm diamond paste. The specimen was mounted on a Ta foil on a 2-axis manipulator, where the crystal could be heated resistively to 1800 K and cooled to 150 K by liquid nitrogen. The crystal temperature was measured by a Pt/Pt-Rh thermocouple spot welded to the edge of the crystal. The preparation of the (1×2) structure followed the procedures described previously.[5,19] The crystal was initially sputtered by argon-ion bombardment for 2 h and subsequently annealed in oxygen atmosphere at 10^{-6} mbar and at temperatures between 900 and 1200 K. A final flash to 1800 K removed the residual oxygen. After different heat treatments in oxygen two different LEED patterns could be observed. The (1×2) superstructure could be obtained after heating the crystal to 900 K in 5×10^{-6} mbar of oxygen for 10 min (Fig. 1). A (1×3) superstructure appeared reproducible after heating the crystal to $\geq$1200 K in 5×10^{-6} mbar of oxygen for $\geq$30 min. At both superstructures no surface impurities could be detected by AES. The sensitivity of the retarding field Auger spectrometer can be estimated to be about 5% of a monolayer. As will be pointed out below, there is evidence that the (1×3) structure, or possibly both structures are stabilized by impurities. However, the preparation of the (1×3) superstructure was reproducible at three different crystals from two different manufacturers.

The crystal could be heated to 1200 K over several hours, without changing the diffraction pattern after cooling. The range over 1200 K has not been tested. Whether the reconstruction remains at 1200 K or has undergone an order-disorder transition as has been observed for Au(110) at 650 K (Refs. 20 and 21) could not be measured. From the directional anisotropy of the surface diffusion it has been suggested that a phase transition should occur around 1000 K.[22] The (1×3) superstructure changes over to the (1×2) reconstruction after heating the crystal at high temperature ($\geq$1800 K) for $\geq$45 min (schematically shown in Fig. 2). The crystal should not be continuously heated to such high temperatures without overheating the copper contacts of the specimen holder. Therefore the crystal was heated to 1800 K for 30 sec after which the system was allowed to cool down for some minutes. The temperature of the contacts was controlled by an extra thermocouple and could be kept below 500 K in order to avoid migration of copper to the platinum crystal. After 80–100 cycles corresponding to a total heating time of approximately 45 min a LEED pattern of a well-ordered (1×2) structure over the whole surface area could be obtained. It is interesting to note

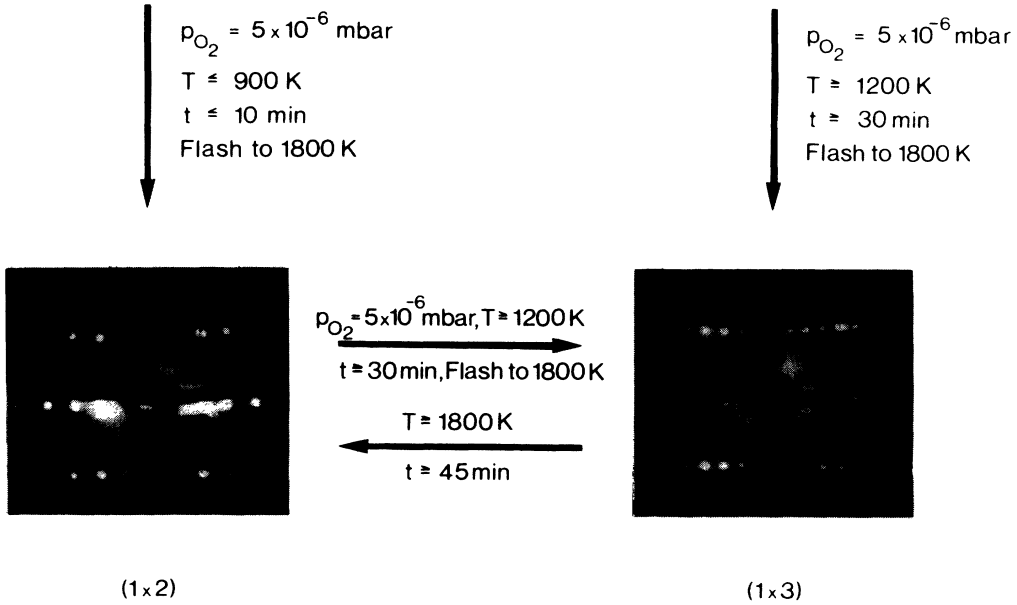

FIG. 1. Preparation of the (1×2) and (1×3) reconstruction of the Pt(110) surface. After an initial argon-ion bombardment a (1×2) or (1×3) reconstruction appears depending on the annealing temperature in an O_2 atmosphere. The (1×2) structure can be obtained from the (1×3) structure only by heating at temperatures above 1800 K for 45 min. LEED patterns are taken at 100 eV.

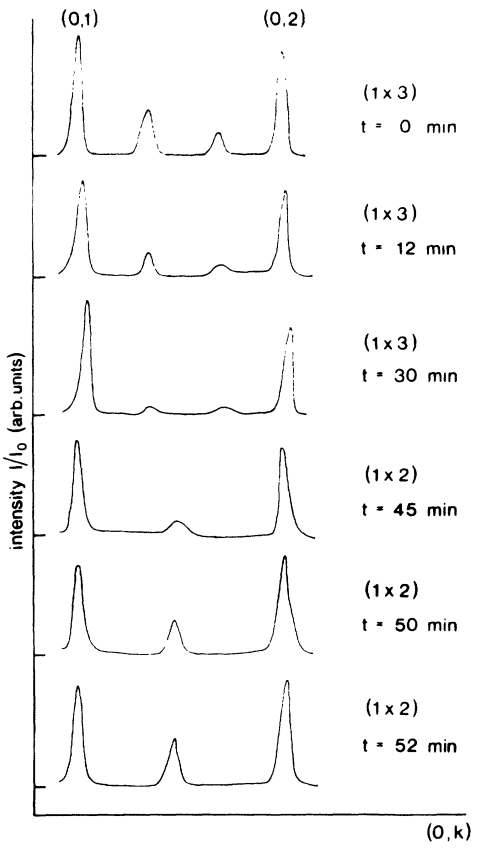

FIG. 2. Transition from the (1×3) structure to the (1×2) structure. The beam profiles for the intermediate stages were taken at room temperature after annealing at 1800 K. The corresponding annealing times are indicated in the figure. An island growth of the (1×2) reconstruction is observed after complete removal of the (1×3) structure.

that at intermediate stages the (1×2) and (1×3) structure coexisted in different parts of the crystal.

The LEED intensity spectra from 12 symmetrically nonequivalent beams of the (1×2) superstructure and 19 symmetrically nonequivalent beams of the (1×3) superstructure at normal incidence in the energy range from 30 to 220 eV were used. Each spectrum was averaged from two or four symmetrically equivalent beams, the background has been subtracted and the intensities were normalized to the incident beam. In most cases only two symmetrically equivalent beams were measurable for geometric reasons. The reproducibility of all beams has been confirmed by repeated measurements after new cleaning procedures. Special care was taken to avoid deviations from normal incidence. The spectra were compared with earlier experimental data[12] to which in most cases only slight differences occurred. In some spectra, however, substantial discrepancies were found. The spectra could also be compared to independent measurements from another experimental group[23] with excellent agreement after careful adjustment of the specimen.

CALCULATION PROCEDURE

The LEED calculations were performed using the layer doubling method[24] and a symmetrized matrix inversion for the interlayer multiple-scattering scheme.[25] The top two layers, and in cases where the interlayer spacing was smaller than 1.3 Å, the first three layers were treated as a compound layer for which the multiple scattering was calculated in angular momentum space. Nine phase shifts were used and the number of the beams in the layer doubling scheme was carefully checked to ensure convergence. It was found that for layer spacings smaller than 1.3 Å the number of beams increased so rapidly that the lattice summation in direct space and the matrix inversion method became more efficient. The crystal potential was obtained from a superposition of relativistically calculated atomic potentials. Similar potentials have been used previously for Au(110) (Ref. 1) and Pb.[26] Further nonstructural parameters in the calculation were an energy dependent imaginary part of the inner potential $V_i = 0.85E^{1/3}$ and a Debye temperature of 270 K for all layers. The energy dependence of the real part of the inner potential has been taken as a fit parameter in the final R-factor analysis assuming a square-root dependence on energy according to a theoretical calculation for the free-electron gas.[27] However, the inclusion of an energy dependent inner potential did nearly not influence the structure parameters.

From the results given by earlier LEED analysis[12] and other methods[3–6] it is evident that the missing-row model provides the best explanation of the (1×2) reconstruction. Therefore, we carried out the calculations for the missing-row model only, without testing again other models. Maintaining the 2-mm symmetry of the surface the missing-row model (Fig. 3) allows an alternate row pairing and buckling in the layers below the top layer. Such relaxations within the first five layers have been included in the structure analysis. In the second and the fourth layer a row pairing was varied in a range from $\Delta y = 0.0$ to 0.2 Å in steps of 0.05 Å. In the third and the fifth layer a buckling from $\Delta z = -0.2$ to 0.2 Å in steps of 0.05 Å was allowed. Together with the first five-layer spacings this resulted in nine free structure parameters which have been varied independently in our calculation.

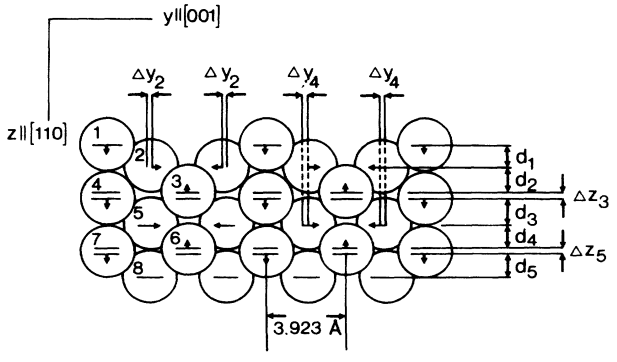

FIG. 3. Missing-row model of the (1×2) reconstruction. The parameters which were optimized in the structure analyses are indicated in the figure. The atoms are numbered as used in Tables I and II.

A block refinement procedure has been used in reaching the minimum. The calculation started with independent variation of three parameters, the two uppermost layer spacings, and a lateral shift in the second layer. These parameters had then been kept fixed and the buckling in the third layer and the third-layer spacing were optimized. The structure parameters in the deeper layers had been subsequently refined, keeping the other parameters fixed. Finally it was checked that the true minimum of all parameters had been reached by repeating the procedure. Except for the interlayer spacing only little correlation between the structure parameters was found. The procedures were similar for the (1×3) structure. Here only four-layer spacings were varied and this resulted in eight independent structural parameters.

(1×2) RECONSTRUCTION

The calculation for the missing-row model resulted in minimum R factors $R_P=0.36$ and $R_{ZJ}=0.26$ (the Pendry[28] and Zanazzi-Jona R factors[29]). Both R factors as a function of a single parameter where all other parameters are kept fixed near their optimum value are displayed in Fig. 4. In nearly all cases the minimum for both R factors is found at the same parameter values within the error limits ensuring the reliability of the structure deter-

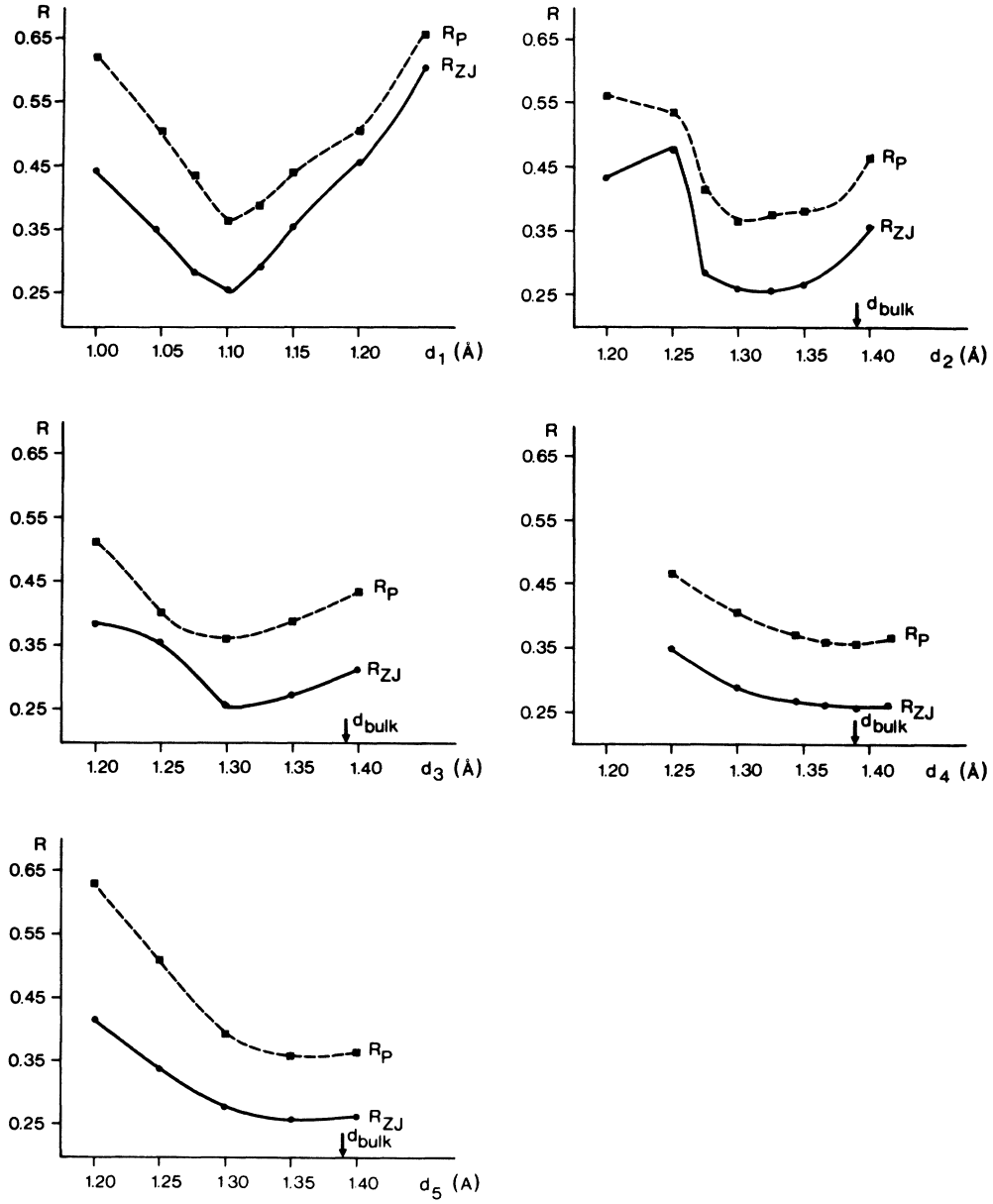

FIG. 4. Averaged R factors for the (1×2) structure as a function of a single structure parameter keeping the other structure parameters fixed at near-optimum values. Dashed line, Pendry R factors; solid line, Zanazzi and Jona R factors.

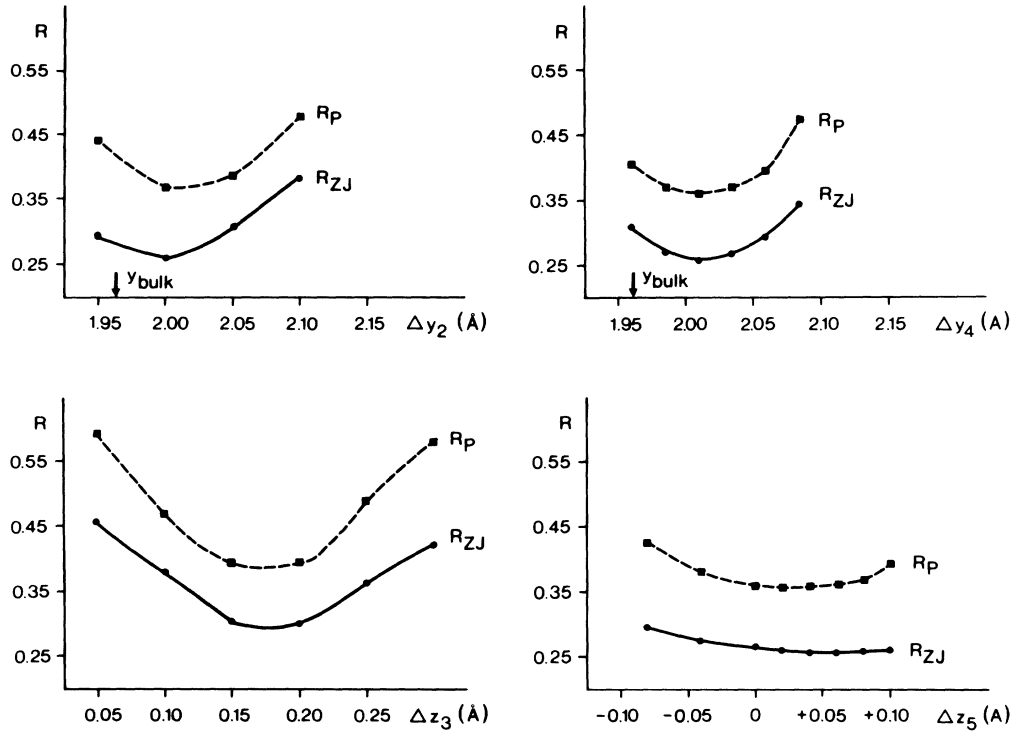

FIG. 4. (*Continued*).

mination. The comparison of the experimental spectra with the calculated spectra is shown in Fig. 5. The values of the best geometrical parameters and the bond lengths between the top six-layer atoms are shown in Tables I and II. A comparison of these results with those found in Pt(110)-(1×2) by energy-minimization calculations[30] shows in general good agreement though some differences in the absolute values of the interatomic relaxations occur. The first three-layer spacings are contracted with respect to the bulk layer spacing. The relaxation of the interlayer spacings quickly vanishes with increasing depths. Relating the layer spacing to the center of the layer, the second- and third-layer spacings are nearly unrelaxed. At the fourth layer a deviation from the bulk value is merely detectable. The contraction of the first-layer spacing which amounts to 0.28 Å is the largest relaxation in this structure and is clearly greater than the value (−0.19 Å) from energy-minimization calculations of Pt(110)-(1×2).[30] The buckling in the third layer $\Delta z_3 = 0.17$ Å is clearly visible, the buckling of the fifth is 0.03 Å and within the error limits of the study. A small lateral shift parallel to the surface has been found in the second (0.04 Å) and the fourth layer (0.05 Å) with nearly the same value. A comparison of our results with those obtained for Au(110)-(1×2) and Ir(110)-(1×2) by LEED structure analysis shows similar relaxations. A clear contraction of the top-layer spacing and further contractions in deeper layer spacings together with a buckling in the third layer is a characteristic in all three cases. However, the Ir(110)-(1×2) surface has a considerably smaller contraction of the first interlayer distance (−12,3%) than Au and Pt (−20,2%).

The deviations from the bulk value for d_4, d_5, Δy_4, and Δz_5 are at the limit of the detectability in the present analysis and cannot be concluded from the minimum of the R factors alone. The R factors $R_{ZJ} = 0.26$ and

TABLE I. Atomic positions for the (1×2) reconstruction in the surface unit cell. The z position with reference to the zero level at the sixth layer and the corresponding bulk values are additionally given.

Atom number	x (Å)	y (Å)	z (Å)	z' (Å)	z_{bulk} (Å)
1	0	0	0	−6.62	−6.95
2	1.39	2.01	1.10	−5.52	−5.56
3	0	3.92	2.39	−4.23	−4.17
4	0	0	2.56	−4.06	−4.17
5	1.39	2.01	3.85	−2.77	−2.78
6	0	3.92	5.23	−1.39	−1.39
7	0	0	5.26	−1.36	−1.39
8	1.39	1.96	6.62	0	0

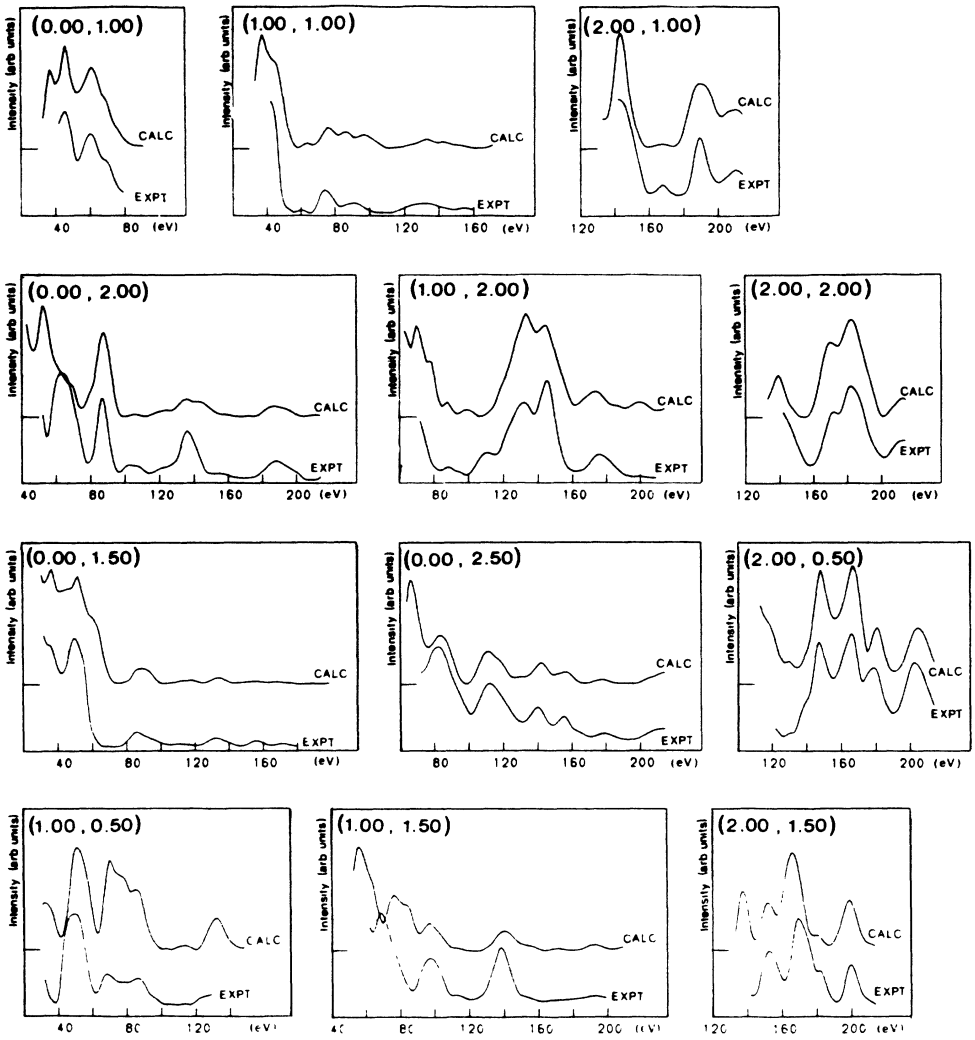

FIG. 5. Experimental and calculated I-V curves for the (1×2) reconstruction. The structure parameters for the calculation are given in Table I.

TABLE II. Interatomic distances for the (1×2) reconstruction and the deviation from the bulk value. The numbering of the atoms is given in Fig. 3.

	r (Å)	Deviation from the bulk value (%)
r_{12}	2.68	−3.2
r_{14}	2.56	−7.6
r_{23}	2.69	−2.9
r_{24}	2.84	+2.5
r_{25}	2.75	−0.7
r_{35}	2.78	+0.4
r_{36}	2.84	+2.5
r_{45}	2.76	−0.4
r_{47}	2.70	−2.5
r_{56}	2.74	−1.1
r_{57}	2.82	+1.8
r_{68}	2.77	±0
r_{78}	2.75	−0.7

$R_P=0.36$ indicate only moderate agreement. Some of the spectra, namely, the (0,2) and (1,1.5) beams, exhibit major discrepancies between the experimental and calculated curves. A large R factor for some beams might increase the error bars such that small relaxations in the deeper layers become undetectable. It has been therefore investigated how much the optimum parameters determined from single beam R factors deviate from the average values. This gives certainly an upper limit of the error bars of the analysis. It has been found that the minima from all beams are relatively close to the average value. The thus determined error bars are about 0.04 Å for the five parameters d_3, d_4, d_5, Δy_4, and Δz_5 and 0.02 Å for d_1 and d_2. Deviations from the bulk value for d_4, d_5, and Δz_5 therefore may be not significant, as already evident from Fig. 4. However, all 12 beams, even those for which the fit is marginal, exhibit a reduction in the R factor by a deviation of these parameters from their bulk values.

Clearly, the agreement between experimental and theoretical spectra is not quite satisfactory though a significant improvement compared to previous studies has been reached. The reason for the remaining discrepancies could not be resolved. Errors in the experimental data due to deviations from normal incidence are certainly too small to explain the large R factors. Specifically the I-V curves of the (0,2) and (1,1.5) beam below 80 eV have been carefully checked and show excellent agreement with an independently taken data set.[23] All structural parameters which possibly could influence the theoretical I-V spectra substantially have been varied in the analysis. Therefore we conclude that nonstructural parameters such as anisotropic thermal vibrations, anisotropic atomic potentials, or different atomic potentials in the surface and bulk layers may be responsible for the remaining misfit. Further reasons may be found in a certain amount of disorder which is always present at these surfaces and becomes visible by a slight broadening of the beams. Small amounts of impurities, as discussed below, can also not be excluded.

(1×3) RECONSTRUCTION

Various models are conceivable for the (1×3) structure. The most likely is a facet model in analogy to the missing-row model. Also, theoretical studies have shown that the Au(110), Ir(110), and Pt(110) surface should have a tendency to form larger (111) facets. The facet model for the (1×3) structure has even been predicted to be energetically favored against the (1×2) structure. However, we tested further models in preliminary calculations, which are referred to as a one missing-row and a two missing-row model. All the three models (Fig. 6) explain the (1×3) reconstruction by missing rows of close-packed atoms in [1$\bar{1}$0] direction. From the three models the facet model (Fig. 7) turned out to be the only one showing agreement between calculated and experimental I-V curves (Fig. 8), and the subsequent structural refinement was performed only for the facet model. The structure refinement of this reconstruction proceeded in the same way as the (1×2) structure analysis. The values of the best geometrical parameters and the bond lengths between the atoms in the top five layers are shown in Tables III and IV. The R factors as a function of a single parameter are displayed in Fig. 9. The final average R factors (19 beams) are $R_P=0.35$ and $R_{ZJ}=0.28$. As for the (1×2) reconstruction, the final R factor is not quite satisfactory though the visual comparison between experimental and theoretical spectral shows in general good agreement. Nearly all details of the experimental spectra are reproduced in the theoretical curves and the agreement is definitely good enough to exclude all other structure models. A deviation from the bulk value for some parameters, namely, the fourth layer spacing d_4, a buckling in the fourth layer Δz_4, and a lateral shift in the third layer Δy_3, are certainly undetectable within the error limits. All other parameters exhibit a significant deviation from the bulk value.

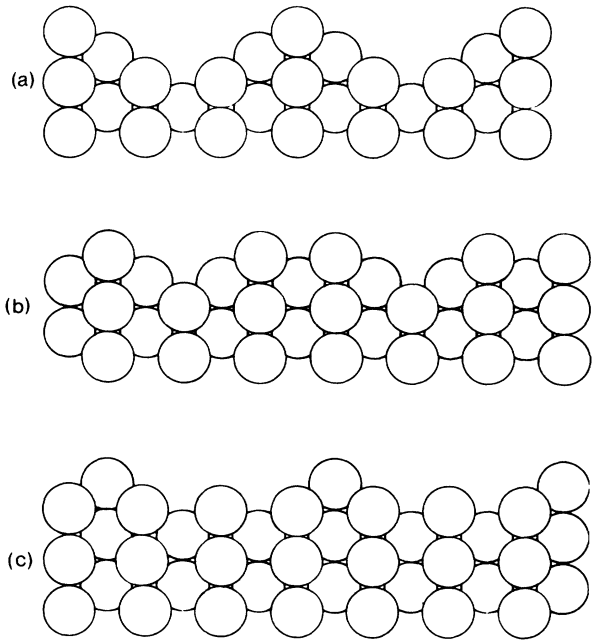

FIG. 6. Three possible models for the (1×3) reconstruction: (a) faceting model, (b) one-missing-row model, and (c) two-missing-row model.

TABLE III. Atomic positions for the (1×3) reconstruction in the surface unit cell. The z position with reference to the zero level at the sixth layer and the corresponding bulk values are additionally given.

Atom number	x (Å)	y (Å)	z (Å)	z' (Å)	z_{bulk} (Å)
1	0	0	0	−5.38	−5.56
2	1.39	2.00	1.10	−4.28	−4.17
3	0	3.93	2.42	−2.96	−2.78
4	0	0	2.60	−2.78	−2.78
5	1.39	5.89	3.96	−1.43	−1.39
6	1.39	1.96	4.00	−1.38	−1.39
7	0	0	5.38	±0	±0
8	0	3.92	5.38	±0	±0

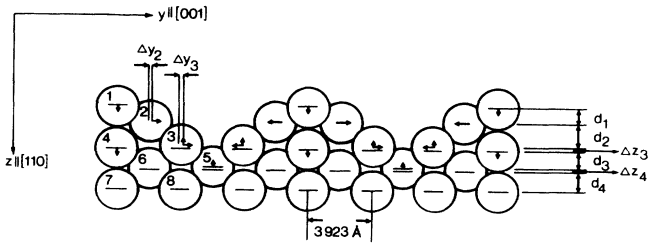

FIG. 7. Facet model of the (1×3) reconstruction with the parameters as used in the analysis.

TABLE IV. Interatomic distances for the (1×3) reconstruction and the deviation from the bulk value. The numbering of the atoms is given in Fig. 3.

	r (Å)	Deviation from the bulk value (%)
r_{12}	2.67	−3.6
r_{14}	2.60	−6.1
r_{23}	2.72	−1.8
r_{24}	2.86	+3.3
r_{35}	2.85	+4.0
r_{36}	2.88	+4.3
r_{38}	2.96	+6.9
r_{46}	2.78	+0.1
r_{47}	2.78	+0.1
r_{58}	2.78	+0.1
r_{67}	2.77	±0
r_{68}	2.77	±0

The result shows a close relation between the (1×2) and (1×3) structure. The (1×3) superstructure has also a clear contraction of the top-layer spacing (−23.2%), a small lateral shift in the second layer (0.05 Å), and a buckling in the third (0.18 Å) layer. A comparison of the interatomic distances in the (1×3) and the (1×2) structure shows that similar contractions occur and that the buckling in the third and fourth layers lead to relative large expansions of interatomic distances between atoms in the third and fourth layer. As in the (1×2) structure the general trend of the atomic relaxations is to smoothen the large corrugation of the surface. The expansion of the distance between the atoms 3 and 5 (Fig. 7) may be uncertain due to the large uncertainty in the determination of the buckling in the fourth layer.

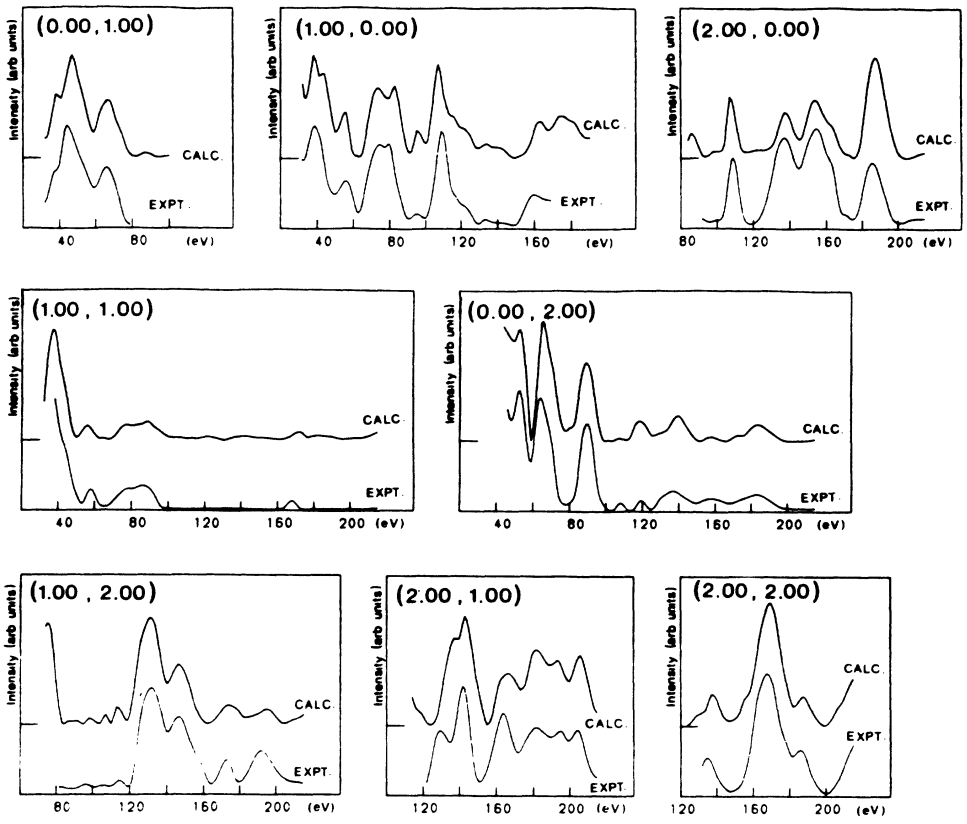

FIG. 8. Experimental and calculated I-V curves of the (1×3) reconstruction. Structure parameters for the calculation are given in Table III.

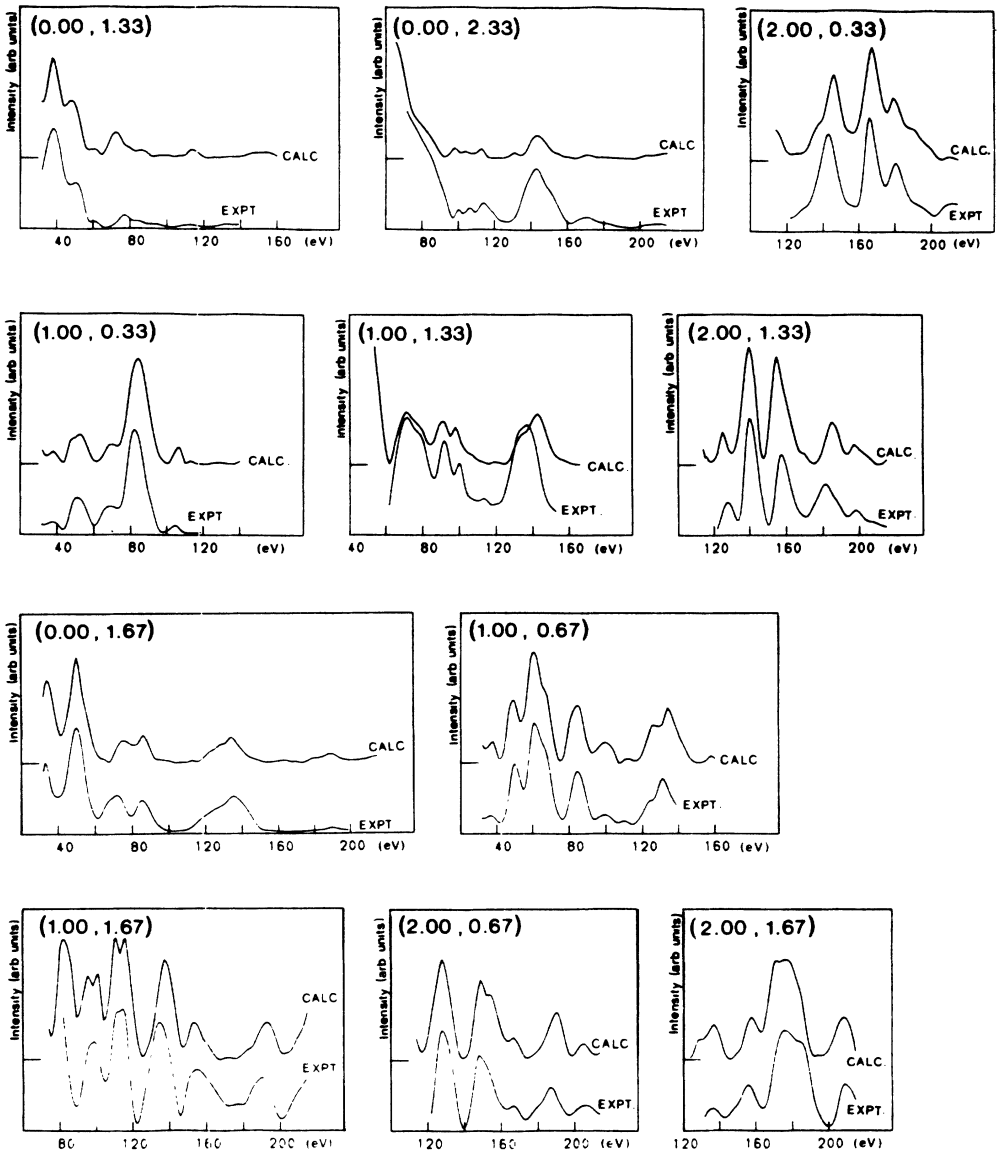

FIG. 8. (*Continued*).

CO-ADSORPTION

In agreement with the results of previous studies[5,6,31] a reversible phase transition (1×2)-(1×1)-(2×1)*p*2*mg* could be observed when the crystal was cooled from 600 to 300 K in 5×10^{-6} mbar CO. The clean (1×2) reconstruction converts at 490 K completely to a disordered (1×1) structure covered with CO. At lower temperatures the (2×1)*p*2*mg* structure appears, which is believed to consist of an unreconstructed substrate lattice and alternatively tilted CO molecules with a coverage $\Theta=1$.[32]

The CO superstructure is complete at 350 K. The reverse process occurs at heating from room temperature to 600 K where the (1×2) reconstruction appears again. This means that the CO adsorption lifts the reconstruction, when CO desorbs at 550 K the (1×2) reconstruction appears again.

The adsorption of CO on the (1×3) structure at the same conditions leads to similar results. First the reconstruction is removed and a presumely disordered (1×1) structure appears and at temperatures below 490 K the intensity of (2×1) superstructure spots start to increase. The *I-V* curves of the (2×1) structure prepared from both reconstructions are identical indicating that there is no difference in the (2×1)/CO structure whether it is prepared from a (1×2) or (1×3) reconstruction. The surprising result is that after desorption of CO at 600 K the (1×3) reconstruction is recovered. The most probable explanation for this behavior is that one of the two reconstructions (or both) is stabilized by impurities. However, no impurities could be detected in the AES. The limits of the detectability of impurities can be estimated to about 0.05–0.01 monolayers.

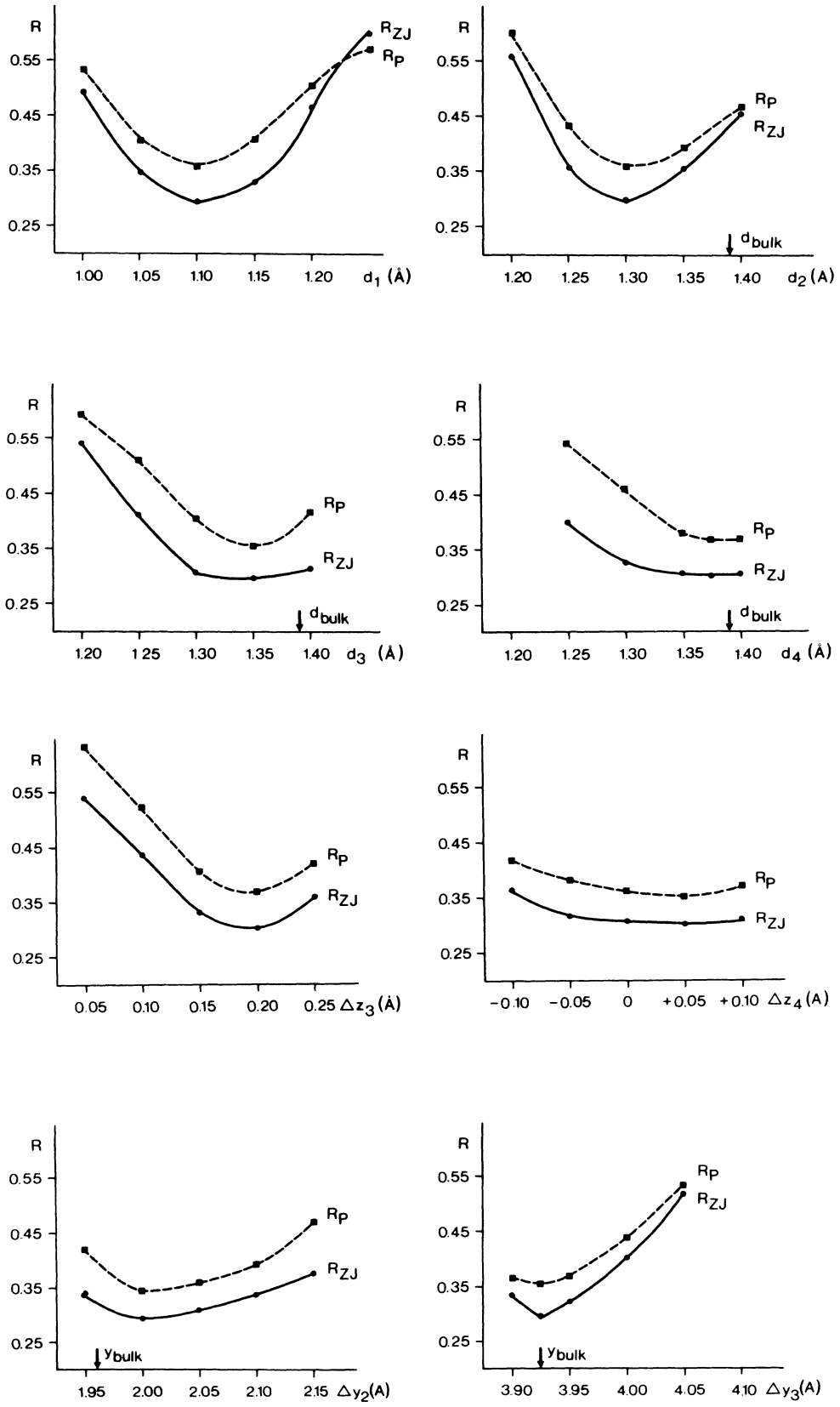

FIG. 9. Averaged R factors for the (1×3) structure as a function of a single structure parameter keeping the other structure parameters fixed at near-optimum values. Dashed line, Pendry's R factors; solid line, Zanazzi and Jona R factors.

DISCUSSION

The origin of the reconstruction of the (110) surfaces of Ir, Pt, and Au and the reason for the existence of well-ordered different reconstructions remains still an unsolved problem after the first discovery about 20 years ago.[33] A theoretical explanation has been tried from several points of view. All calculations favor clearly the missing-row structure over alternative models[34] though structural details like magnitude and direction of distortions in subsurface layers are not always in agreement with experimental results.

A redistribution of the electronic density from the repulsive *d* bands to the attractive *s-p* bands in the surface region has been discussed recently by Heine and Marks.[35] It has been argued that in the surface the electronic density in the *s-p* bands increases while the density of states in the *d* bands decreases. This causes a tendency towards smaller interatomic distances because the potential minima for the *s-p* and *d* bands differ substantially. These arguments seem plausible and give qualitatively a correct picture though the direction of the atomic relaxations depends sensitively on the parameters used in the calculation. This picture has also been recently confirmed by total energy calculations for Au(110) using a pseudopotential approach within the local-density functional formalism.[36] Further support for this picture comes from the proof that the (1×2) reconstruction of Ag(110) induced by adsorbed potassium is also of the missing-row type.[37] A different approach from total energy calculations within the effective medium theory has been described by Jacobson and Nørskov.[17] The properties of the surface are related here to bulk properties like the shear modulus and the compressibility. In these calculations a clear preference for the missing-row model is found and the existence of (1×3) and (1×4) reconstructions has also been predicted. However, because of the small difference in total energy between the (1×2) structure and the higher-order reconstructions one should expect that the surface is disordered and that the entropy term of the total energy should cause a simultaneous occurrence of all periodicities and a continuous transitions from the (1×2) reconstruction to higher-order reconstructions. Such disorder has been indeed directly observed in the STM picture on Au(110) (Ref. 7) and has been also determined from a beam profile analysis of Au(110).[21] In the present case it was found that both structures are rather well ordered. No indications for a continuous transition between the two structures could be detected. This is an additional indication that one of the structures is not a stable configuration of the clean surface.

Total energy calculations have been also performed by Daw for Pt(110).[30] The structural parameters found there are in good agreement with our findings. A comparison between experimental and theoretical data also for Ir and Au surfaces has been recently given by Chan and Van Hove.[2] A somewhat different approach but also from total energy calculations has been described by Tomanek *et al.*[38] for Pt(110). The results favor also the missing-row model but cannot describe the larger superstructures. The reconstruction has been also found energetically favorable for Au(110) using pair-potential and many-body correction terms.[18] A possible relationship between the anisotropy of the surface energy and the surface reconstruction has been discussed recently in detail.[39] It was found that the anisotropy of the surface free energy is high enough to favor a faceting, that means that indeed the stability of the (111) face can be seen as the reason for the reconstruction. However, the high degree of disorder typically present at faceted surfaces is missing in the (1×2) and (1×3) structures so that this point still remains to be explained.

The existence of two reconstructions leads to the question which of the two reconstructions is the stable surface structure. Because the formation of the stable structure may be kinetically inhibited it would be highly interesting to know the mechanism of the reconstruction. The reconstruction involves the movement of many atoms, which cannot be explained by the jumping of surface atoms across one row of atoms since the activation energy for this process is much too large to be consistent with the observed transition temperature. The (1×1)→(1×2) phase transformation occurs at 300 K within about a minute and a mechanism of the reconstruction has been explained by cross-channel diffusion involving two atoms[40–43] or alternatively by diffusion along the [1$\bar{1}$0] rows. Assuming a cross-channel diffusion mechanism a transition from the (1×1) structure to the (1×3) structure should be even favored against a (1×1)→(1×2) transition because the (1×3) structure is easily obtained from a (1×1) structure by one diffusion step for every third row. No diffusion over a long distance is required. It would be therefore interesting to study the kinetics of a possible (1×1)-(1×3) phase transformation. That a metastable (1×1) structure can be prepared from a (1×2) structure has been already demonstrated.[31] The preparation of a metastable (1×1) structure starting from a (1×3) structure by CO adsorption and subsequent desorption by electron bombardment should therefore be possible, too. A (1×1)→(1×3) transition should be also observable during thermal CO desorption but has not yet been experimentally verified. That such a transition is usually not observed indicates once more that the (1×3) structure is stabilized by impurities. The high temperatures which are necessary to restore the (1×2) structure from the (1×3) structure are too high to be explainable by an activation barrier for a surface diffusional process. From this argument and the observation that the (1×3) structure is recovered after CO adsorption and desorption we conclude that the (1×3) does not correspond to a stable surface structure of the clean surface.

Interpretation of the structure data shows for both surfaces that a clear contraction of the interatomic distances along the surface exists, i.e., d_{12}, d_{23}, etc. are smaller than in the bulk. This may be connected with a reconstruction in reducing the surface energy. The buckling and slight lateral shifts found in the subsurface layers are a consequence of the corrugation of the surface and the tendency of the electron density to smoothen the corrugation. These relaxations are similar to multilayer relaxations found in clean metal surfaces[44] and cause a buck-

ling here because of the doubled and tripled periodicity. The general picture found here resembles closely the results for interlayer relaxations in clean metal surfaces.

ACKNOWLEDGMENTS

The authors wish to thank Dr. Y. Gauthier for making his experimental data available for comparison with our results and valuable experimental hints. We thank also Professor H. P. Bonzel and Dr. D. L. Adams for stimulating discussions and H. Antesberger, H. Huber, and H. Plöckl for technical assistance. Financial support by the Deutsche Forschungsgemeinschaft (Sonderforschungsbereich No. 128) is gratefully acknowledged.

[1]W. Moritz and D. Wolf, Surf. Sci. **163**, L655 (1985).
[2]C.-M. Chan and M. A. Van Hove, Surf. Sci. **171**, 226 (1986).
[3]G. L. Kellog, Phys. Rev. Lett. **55**, 2168 (1985).
[4]N. Niehaus, Surf. Sci. **145**, 407 (1984).
[5]T. E. Jackmann, J. A. Davies, D. P. Jackson, W. N. Unertl, and P. R. Norton, Surf. Sci. **120**, 389 (1982).
[6]D. P. Jackson, T. E. Jackmann, J. A. Davies, W. N. Unertl, and P. R. Norton, Surf. Sci. **126**, 226 (1983).
[7]G. Binning, H. Rohrer, Ch. Gerber, and E. Weitel, Surf. Sci. **131**, L379 (1983).
[8]M. Copel and T. Gustafsson, Phys. Rev. Lett. **57**, 723 (1986).
[9]J. Möller, K. J. Snowdon, W. Heiland, and H. Niehus, Surf. Sci. **178**, 475 (1986).
[10]H. Hemme and W. Heiland, Nucl. Instrum. Methods B **9**, 41 (1985).
[11]I. K. Robinson, Phys. Rev. Lett. **50**, 1145 (1983); I. K. Robinson, Y. Kuk, and L. C. Feldman, Phys. Rev. B **29**, 4762 (1984).
[12]D. L. Adams, H. B. Nielsen, M. A. Van Hove, and A. Ignatiev, Surf. Sci. **104**, 47 (1981).
[13]W. Moritz and D. Wolf, Surf. Sci. **88**, L29 (1979).
[14]K. Christmann and G. Ertl, Z. Naturforsch. **28a**, 1144 (1973).
[15]M. Salmeron and G. A. Somorjai, Surf. Sci. **91**, 373 (1980).
[16]M. Mundschau and R. Vanselow, Phys. Rev. Lett. **53**, 1085 (1984).
[17]K. W. Jacobsen and J. K. Nørskov, in *The Structure of Surfaces II,* edited by J. F. van der Veen and M. A. Van Hove (Springer-Verlag, Berlin, 1987), p. 118.
[18]M. Garofalo, E. Tosatti, and F. Ercolessi, Surf. Sci. **188**, 321 (1987).
[19]H. P. Bonzel and R. Ku, J. Vac. Sci. Technol. **9**, 663 (1972).
[20]D. Wolf, H. Jagodzinski, and W. Moritz, Surf. Sci. **77**, 265 (1978).
[21]J. C. Campuzano, M. S. Forster, G. Jennings, R. F. Willis, and W. Unertl, Phys. Rev. Lett. **54**, 2684 (1985).
[22]N. Freyer and H. P. Bonzel, Surf. Sci. **160**, L501 (1985); H. P. Bonzel, N. Freyer, and E. Preuss, Phys. Rev. Lett. **57**, 1024 (1986); E. Preuss, N. Freyer, and H. P. Bonzel, Appl. Phys. A **41**, 137 (1986).
[23]Y. Gauthier (private communication).
[24]M. A. Van Hove and S. Y. Tong, *Surface Crystallography by Low Energy Electron Diffraction* (Springer, Berlin, 1979).
[25]W. Moritz, J. Phys. C **17**, 353 (1984).
[26]W. Hösler, W. Moritz, E. Tamura, and R. Feder, Surf. Sci. **171**, 55 (1986).
[27]L. Hedin and B. I. Lundquist, J. Phys. C **4**, 2064 (1971).
[28]J. B. Pendry, J. Phys. C **13**, 937 (1980).
[29]E. Zanazzi and F. Jona, Surf. Sci. **62**, 61 (1978).
[30]M. S. Daw, Surf. Sci. **166**, L161 (1986).
[31]S. Ferrer and H. P. Bonzel, Surf. Sci. **119**, 234 (1982).
[32]D. Rieger, R. D. Schnell, and W. Steinmann, Surf. Sci. **138**, 361 (1984).
[33]D. G. Fedak and N. A. Gjostein, Acta Met. **15**, 827 (1967).
[34]H. P. Bonzel and S. Ferrer, Surf. Sci. **118**, L263 (1982).
[35]V. Heine and L. D. Marks, Surf. Sci. **165**, 65 (1986).
[36]K.-M. Ho and K. P. Bohnen, Phys. Rev. Lett. **59**, 1833 (1987); Europhys. Lett. **4**, 345 (1987).
[37]J. W. M. Frenken, R. L. Krans, J. F. Van der Veen, E. Holub-Krappe, and K. Horn, Phys. Rev. Lett. **59**, 2307 (1987).
[38]D. Tomanek, H.-J. Brocksch, and K. H. Bennemann, Surf. Sci. **138**, L129 (1984).
[39]H. P. Bonzel and K. Dückers, *Chemistry and Physics of Solid Surfaces 7* (Springer, Verlag, in press).
[40]S. H. Garofalini and T. Halicioglu, Surf. Sci. **112**, L775 (1981).
[41]S. H. Garofalini and T. Halicioglu, Surf. Sci. **104**, 199 (1981).
[42]H. P. Bonzel, Surf. Sci. **121**, L531 (1982).
[43]S. H. Garofalini and T. Halicioglu, Surf. Sci. **121**, L535 (1982).
[44]K. Heinz, Appl. Phys. A **41**, 3 (1986), and references therein.

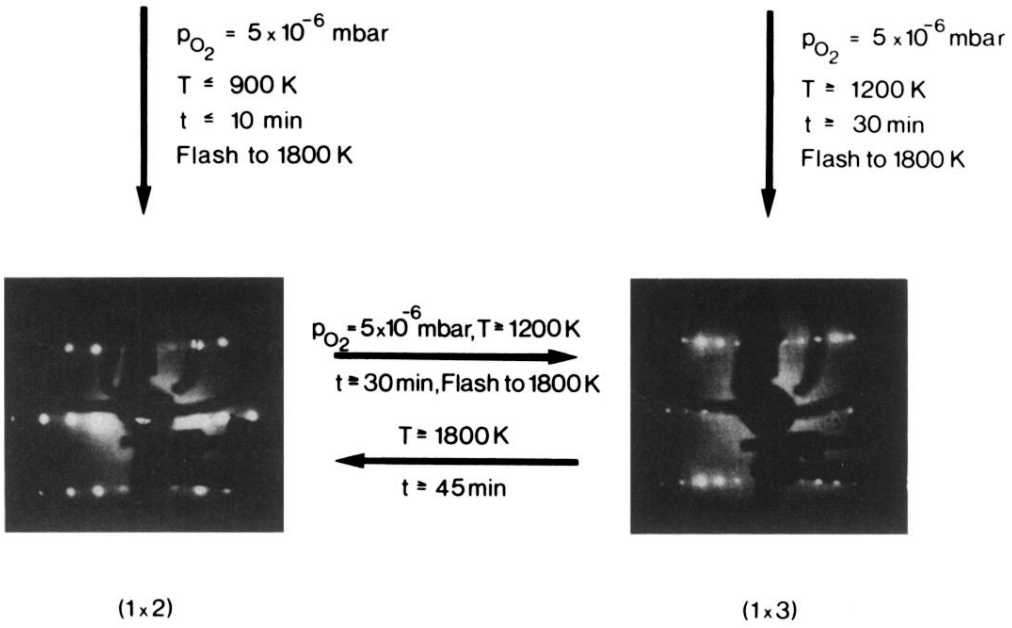

FIG. 1. Preparation of the (1×2) and (1×3) reconstruction of the Pt(110) surface. After an initial argon-ion bombardment a (1×2) or (1×3) reconstruction appears depending on the annealing temperature in an O_2 atmosphere. The (1×2) structure can be obtained from the (1×3) structure only by heating at temperatures above 1800 K for 45 min. LEED patterns are taken at 100 eV.